PHYSICAL REVIEW C VOLUME 18, NUMBER 1 JULY 1978

Implications for statistical theories of fragmentation from measurements of Ag(p,^{3}He) and Ag(p,^{4}He) at intermediate proton energies

Ray E. L. Green and Ralph G. Korteling
Department of Chemistry, Simon Fraser University, Burnaby, British Columbia, Canada V5A 1S6
(Received 27 December 1977)

Energy spectra and angular distributions measured for ^{3}He and ^{4}He emitted from an Ag target bombarded with 210, 300, and 480 MeV protons are analyzed in terms of rapidity and relativistically invariant cross section. This analysis yields constraints on the possible velocities of any systems assumed to be deexciting by statistical processes. Constraints on the masses of emitting systems follow from kinematics, with implications for statistical theories: e.g., independent of the model used, the concept of evaporation is shown by this analysis to be insufficient to explain all of the data.

[NUCLEAR REACTIONS Ag(p,^{3}He), (p,^{4}He), E=210, 300, 480 MeV; θ=20, 90, 160°; measured $\sigma(E, E_{He}, \theta)$. Invariant cross section, rapidity analysis; deduced nonevaporation components, constraints on statistical theories.]

INTRODUCTION

For over a decade it has been apparent that existing calculations based on the evaporation process do not adequately explain the data on fragmentation products from nuclei bombarded with medium and high energy protons.[1-4] Various models of additional mechanisms, some statistical and others direct, have been invoked in an effort to explain the data not accounted for by the evaporation calculations.[4-9] The justification for these additional mechanisms has, however, often rested on the inadequacies of specific model calculations of evaporation. Improvements in evaporation models and calculations have at times significantly reduced previous discrepancies, for example see Ref. 3 or 15.

It is therefore important to determine whether the conventional evaporation mechanisms are appropriate or not. By suitably modifying analysis techniques recently applied in relativistic heavy-ion work,[10] a model-independent procedure has been formulated to indicate which portions of fragment spectra can and cannot be explained by these evaporation mechanisms.

Helium isotopes have been chosen for this study because large differences in the evaporation probabilities of ^{3}He and ^{4}He are expected and observed. The ^{4}He spectra are dominated by a component which is easily interpreted as due to evaporation, while the ^{3}He spectra are difficult to explain in such terms. In addition, the intermediate energy interactions of 200 to 500 MeV protons on a silver target are well suited to study this problem since they yield more tractable kinematic limits than the previous work conducted with GeV protons.[1-3]

This article will show that the model-independent analysis presented here, coupled with kinematic limits from the moderate incident proton energies, can give direct information on the mechanisms responsible for He fragment emission. Not only does it show that a significant fraction of the ^{4}He spectra as well as the majority of the ^{3}He spectra cannot be due to a conventional evaporation mechanism, but it also indicates the range of source velocities which any statistical theory must incorporate if it is to explain the fragment emission.

EXPERIMENTAL DATA AND DATA REDUCTION

The data used in this article were taken with standard transmission silicon surface barrier detectors mounted in a scattering chamber at the TRIUMF accelerator. Most of the relevant experimental procedures are outlined elsewhere.[11] At each of the proton energies involved, an absolute normalization of the data was obtained by relating the counting rate for 40 to 80 MeV ^{4}He fragments in a monitor counter at 90° to the counting rate from proton elastic scattering in a polarimeter[12] mounted in the proton beam line approximately 1.5 m beyond our target. These absolute normalizations should be correct to ± 25%, while our internal relative normalizations at a given energy should be within the error from the statistics of counting (usually < 1%) plus a 4% uncertainty due to the limited accuracy to which the energy windows on the ^{4}He can be set. (In those cases where there are identical runs separated in time by several months, the differences in relative normalizations have been within this error.)

The targets used were 2.3 mg/cm^2 natural silver and approximately 100 μg/cm^2 VYNS film which was used to obtain a correction for light mass impurities on the Ag target. This correction is included in our spectra but is of negligible importance to the analysis presented here. Corrections to the He energy spectra from the finite Ag target thickness are also of negligible importance in the analysis here and have been applied only to model evaporation calculations.

The main data telescope used consisted of four data detectors of increasing thickness (12.9, 76, 476, and 1065 μm) followed by a veto counter for particles not stopping in the detector stack. The measured fragment energy ranges were extended by use of 319 and 639 mg/cm^2 aluminum absorbers in front of this telescope. Identification of the fragments followed procedures previously described[11] using the 76 μm detector for ΔE (considering the 12.9 μm detector as part of the absorber), except for the lowest energy fragments where the 12.9 μm detector was used for ΔE. The $\Delta E, E$ identification of ^{3}He and ^{4}He with the 76 μm ΔE is essentially unambiguous; 10 to 1 to 300 peak-to-valley-to-peak is seen in typical particle identification (PI) spectra. The identification of ^{3}He with the 12.9 μm ΔE in the low energy region is complicated by the inherent decrease in PI resolution with thin detectors coupled with a dramatic increase of ^{4}He relative to ^{3}He at low energies; for equal ^{3}He and ^{4}He peaks in PI spectra from absorber modified data, 3 to 1 to 3 ratios are seen. Since our target contaminant correction is also no longer negligible for ^{3}He at the lowest energies, we have not included ^{3}He data below 10 MeV in the analysis undertaken in this article.

DATA ANALYSIS

An interesting method for analyzing fragment spectra measured in relativistic heavy-ion studies has been published recently.[10] We feel the method is also well suited for analysis of proton induced fragmentation, leading easily to some conclusions not readily apparent in more conventional treatments of fragment data.

Rather than using the ordinary inclusive double differential fragment cross sections and fragment energies, we work with the fragment momentum p and the relativistically invariant cross section

$$f = \frac{1}{p}\frac{d^2\sigma}{d\Omega\, dE}\,.$$

Typical fragment spectra then appear as in Fig. 1. The solid curve is drawn through the data to expedite and smooth the remaining analysis. The

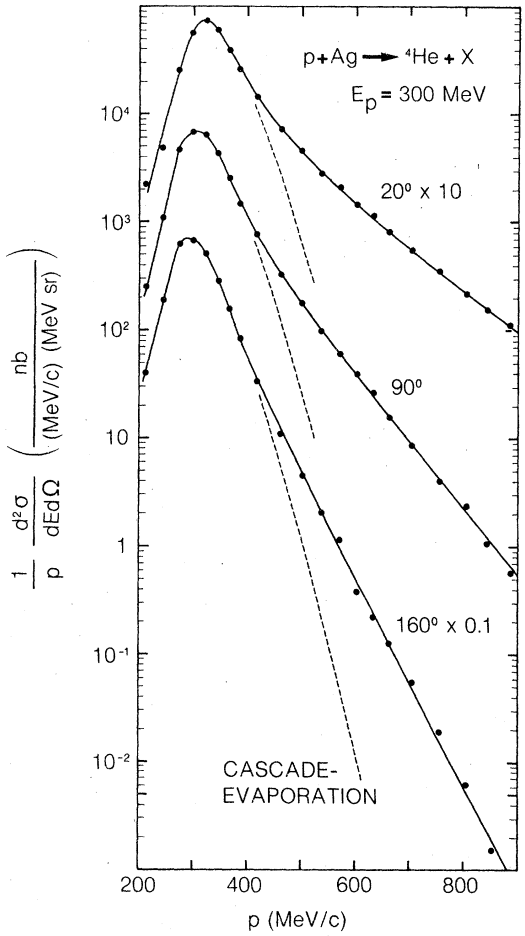

FIG. 1. Relativistically invariant cross section versus fragment momentum for ^{4}He fragments from 300 MeV protons incident on Ag. Relative errors are generally less than or approximately equal to the size of the points. The dashed curve is the sample cascade-evaporation calculation discussed in the text; in the region of the maxima, it is indistinguishable from the solid curve drawn through the data.

dashed curve is typical of our best cascade-evaporation results from a calculation similar to one described previously.[3] This calculation assumes that the excited residual nuclei resulting from an initial cascade have Maxwellian distributions of excitation energy and that the forward momentum of a residual nucleus is proportional to its excitation energy. The principal difference from the previous calculation is the use of a better inverse compound nucleus cross section calculation.[13] The details of this sample calculation are unimportant to the remaining analysis; it is not necessarily the final description of the evaporation component and has been included merely to point up one of the questions being addressed by this article.

From the detector angle and the invariant cross

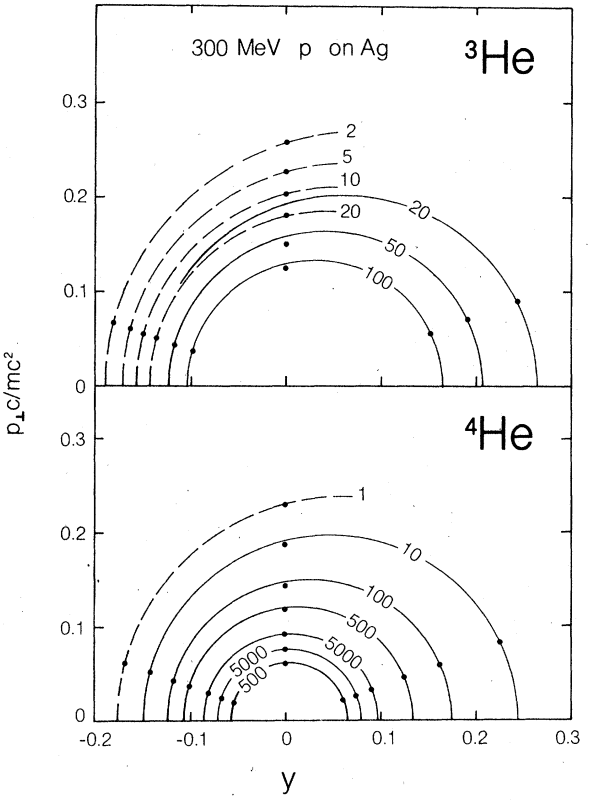

FIG. 2. Sets of data points of constant invariant cross section in the $(y, p_\perp c/mc^2)$ plane for ^{3}He and ^{4}He fragments from 300 MeV protons incident on Ag; $p_\perp$ is the transverse momentum of the fragment, m is its mass, and $y = \frac{1}{2}\ln[(W+p_\parallel c)/(W-p_\parallel c)]$ is its rapidity, where W is the fragment total energy. Fits for isotropic emission from sources moving in the beam direction are shown with labels indicating invariant cross section in nb/[(MeV/c)(MeV sr)]. Solid circular curves are fits to 20° and 160° data points; dashed circular curves are fits to 90° and 160° data points.

section spectra, we obtain sets of values of the fragment's perpendicular momentum $p_\perp$ and rapidity y at constant values of the invariant cross section. The rapidity variable[14]

$$y = \tfrac{1}{2}\ln[(W+p_\parallel c)/(W-p_\parallel c)],$$

where W is the total energy of the fragment including its rest mass energy, has the convenient property that it merely changes by a constant value if expressed in a frame moving in the beam direction. For our data, it is convenient to carry the normalization of $p_\perp$ a step further than Ref. 10 by using $p_\perp c/mc^2$, where m is the fragment mass, since the two variables being used then become the fragment's parallel and perpendicular velocities (in units of c) in the nonrelativistic limit. Although in fact our data are essentially nonrelativistic, the relativistic quantities are used because their explicit transformation properties are very convenient.

Figure 2 shows a selected set of data points of the type described in the preceding paragraph for the cases of ^{3}He and ^{4}He fragments from 300 MeV protons incident on a silver target. Solid circular contour lines centered about the rapidity axis are shown connecting 20° and 160° data points with the same invariant cross section; dashed circular contour lines are shown connecting 90° and 160° data points with the same invariant cross section. For these plots, a change of reference frame from the laboratory to any other frame moving in the beam direction merely shifts the rapidity axis by a fixed amount, all other quantities being relativistically invariant.

The value of plots like Fig. 2 when working with distributions likely to have significant contributions from statistical reaction sources becomes clear from the following: Excited nuclei with rapidity ϵ statistically deexciting by emission of a given fragment would result in contours on plots such as Fig. 2 which were symmetric about $y = \epsilon$. If the emission was isotropic, such contours would be, in the nonrelativistic limit, circles centered about $y = \epsilon$. In this simple case of fixed source rapidity, the quantity $v = \epsilon c$ is merely the source velocity (nonrelativistically) as used in numerous previous discussions of fragment emission and target recoil experiments.

To the detriment of simplicity, in fragmentation reactions almost all quantities involved are distributed over a range of values which leads to complications that cannot be lightly regarded. This means that one cannot, for example, directly associate the value s, about which an experimentally determined contour of constant invariant cross section f happens to be symmetric, with a unique value ϵ of emitting system rapidity. Nor, for that matter, can one associate the contour with a unique source mechanism.

In spite of the preceding reservations, plots of s as just defined versus f are very instructive, allowing one to draw both analytically sound and speculative conclusions. Two sets of such plots are shown in Fig. 3 for ^{3}He and ^{4}He from 210, 300, and 480 MeV protons incident on silver. The upper curves are s versus f, where s is the point about which an isotropic distribution passing through the 20° and 160° data points would be centered; the lower curves are s' versus f, where s' is the point about which an isotropic distribution passing through the 90° and 160° data points would be centered. The cutoff in the maximum value of f for these curves is $0.9\times f_{\max}(160°)$ because analysis of this nature becomes sensitive

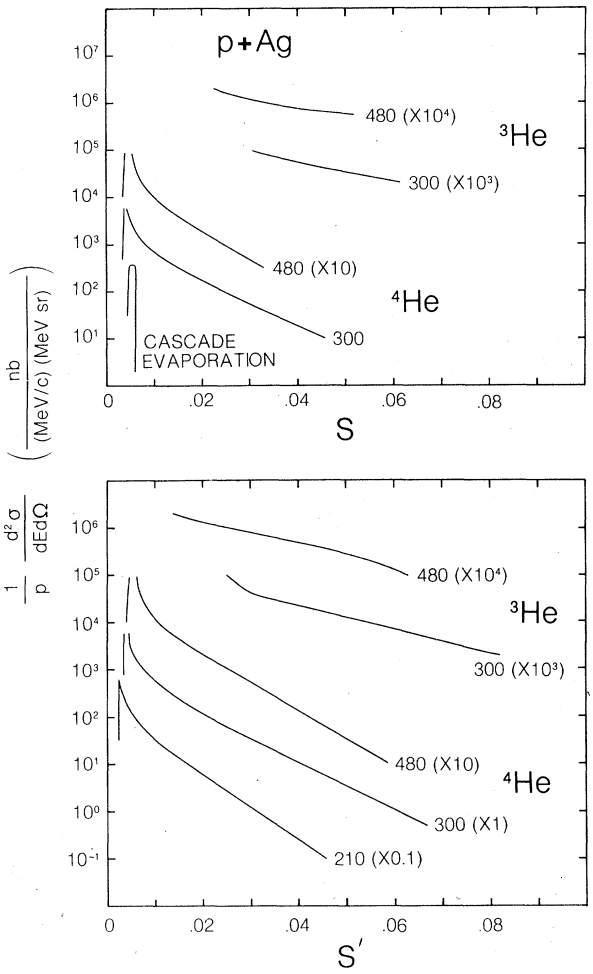

FIG. 3. Invariant cross section versus source rapidity as defined by fitting isotropic distributions from moving sources to data points of the given invariant cross section (as in Fig. 2) for ^{3}He and ^{4}He from 210, 300, and 480 MeV protons incident on Ag. Source rapidities based on 20° and 160° data points are called s and those based on 90° and 160° data points are called s'. An arbitrarily normalized curve is shown for a typical evaporation calculation for ^{4}He from 300 MeV protons in which distributed excitation energies and forward momenta are used for the residual system formed by the cascade.

to experimental errors near the maximum in invariant cross section. The lower terminations on f are determined by the value of $f(20°)$ or $f(90°)$ at the highest and lowest values of fragment momentum for which we have determined f with sufficient accuracy for this analysis. The two sets of curves for ^{4}He are essentially identical at low values of s and s', a reflection of the isotropic appearance of the contours in Fig. 2 for low ^{4}He momentum. The curves begin to diverge slightly before the 20° data are cut off, a reflection of the slight nonisotropy seen in Fig. 2 at high ^{4}He momentum. The two sets of ^{3}He curves have different values everywhere, reflecting the nonisotropy of the ^{3}He data. As is reasonable, the ^{4}He curves indicate increasing source rapidities for increasing beam energies in the high cross section region where evaporation from a moving residual source is expected to be the dominant process.

Interpretation of other aspects of these curves is complicated by the previously mentioned difficulty of associating s or s' with a unique source rapidity ϵ. However, if one assumes the observed invariant cross section is due to an integral over the product of the distribution of source rapidities involved in fragment emission and a function at each source rapidity symmetric about the source rapidity, the data imply that the distribution of source rapidities is somewhere nonzero at or beyond the maximum values for s in Fig. 3. While a somewhat more detailed connection between s and source rapidities may be possible for the case of symmetric fragment emission, the above conclusion is sufficient to place significant constraints on statistical theory models purporting to explain the data.

IMPLICATIONS FOR STATISTICAL THEORIES

Among other consequences, the conclusion of the preceding paragraph is sufficient to rule out standard evaporation concepts as an explanation for the entirety of our data. If our data were all due to evaporation from equilibrated nuclear species, one would expect fragment emission symmetric about 90° in the frame of the emitting nucleus. Consequently, we would then have to conclude that the laboratory rapidities of the emitting nuclei extend beyond, for example, $\epsilon = 0.06$. At our proton incident energies, this kind of emitting system rapidity implies severe constraints on the mass of the emitting system. Based purely on kinematics, for example, a 100 MeV ^{4}He fragment (approximately corresponding to a contour in Fig. 2 centered about $y = 0.06$) from 300 MeV protons on ^{109}Ag could be evaporated from a nucleus of $\epsilon = 0.06$ only if the mass of this nucleus was $A_\epsilon \leq 64$ (with equality only for the very improbable case that all other particles were emitted exactly backwards with identical c.m. velocities). Under a more reasonable physical assumption that the emitting system momentum is less than or equal to the incident proton momentum, one finds $A_\epsilon \leq 14$ for $\epsilon = 0.06$. Clearly these emitting masses require mass removals in the cascade step of the cascade-evaporation model which are not compatible with any standard concepts of these processes. This result is important because of its model-indepen-

dent nature; it is not surprising since the various attempts[1-4] to explain heavy fragments produced from high-energy proton bombardments on the basis of evaporation invariably have failed to explain all portions of the data. The source of this failure, as explained above, is illustrated in Fig. 3 where the same cascade-evaporation calculation used in Fig. 1 is shown, here with arbitrarily displaced magnitude.

The isotropic appearance of the ^{4}He data suggests that it may be profitable to be less rigorous and examine the implications of associating the measured curves of Fig. 3 with emitting system rapidities, and then associating these, under some reasonable assumptions about the momentum transfer from the proton to the residual system, with a mass distribution of these residual systems. This mass spectrum for the emitting systems ranges from near the target mass down to a few times the fragment mass. The light mass emitting systems are predominantly associated with high-energy fragments but are not believed to be due to evaporation from true light nuclei because we do not observe the additional cross section below the silver region Coulomb barrier cutoff that would be implied from attributing the high-energy cross section to light nucleus evaporation.

One possible interpretation of such a range of masses involved in fragment emission is that the incident proton has an initial interaction involving a few nucleons which then interact with ever increasing numbers of other nucleons until the energy is distributed amongst all nucleons remaining in the system and that fragment emission can take place from the subset of interacting nucleons at any point between the initial and final points. This scheme views the nonevaporation source of fragments as a fast but statistical process, a very different kind of preequilibrium decay than conceived of in typical exciton models[8] which suffer the same fate as evaporation when the analysis in this article is applied to them. This kind of idea has been suggested previously[1] and encouraging results have been obtained for 600 MeV protons incident on various targets with a two point approximation to this concept where, in addition to evaporation, fragments are considered to arise in the initial interaction of the proton with a small subset of the target nucleons via Hagedorn statistical thermodynamics.[4]

Other models, such as quasifree scattering off various momentum components of preformed clusters[9] are of course not automatically ruled out by this analysis. On the other hand, they do not automatically give rise in any obvious way to the observed features in Fig. 2 and 3.

CONCLUSIONS

In summary, analysis of fragment emission data in terms of contours of relativistically invariant cross section in a plane of rapidity versus $p_\perp c/mc^2$ provides a convenient graphic representation of the data, which succinctly displays the important features. Model-independent information on source velocities is obtained from such an analysis and this can be of value at the conceptual stage when choosing between possible model calculations. Such plots may also be used to readily identify areas where more data are needed to suggest the proper shape of these contours, e.g., for our ^{3}He cases it would clearly be beneficial to have more angular information. For the ^{4}He cases, it appears that the most interesting information would come from extending the upper end of the energy range. Either suggested extension of the data would help choose between alternate mechanisms being proposed as an explanation of nonevaporation fragments. The study of heavier fragments should also be beneficial in this regard.

ACKNOWLEDGMENTS

This work was supported by the National Research Council of Canada. The authors greatly appreciate a critical reading of the manuscript and helpful suggestions by K. P. Jackson. We acknowledge with thanks the help received from the operations staff of TRIUMF in obtaining the proton beams used in this experiment.

[1] A. M. Poskanzer, G. W. Butler, and E. K. Hyde, Phys. Rev. C 3, 882 (1971).
[2] E. K. Hyde, G. W. Butler, and A. M. Poskanzer, Phys. Rev. C 4, 1759 (1971). The Introduction in this paper and its references provide a good review of previous work.
[3] R. G. Korteling, C. R. Toren, and E. K. Hyde, Phys. Rev. C 7, 1611 (1973).
[4] J. P. Alard *et al.*, Nuovo Cimento A30, 320 (1975) (Hagedorn thermodynamics).
[5] S. T. Butler and C. A. Pearson, Phys. Rev. 129, 836 (1963). H. H. Gutbrod *et al.*, Phys. Rev. Lett. 37, 667 (1976) (coalescence).
[6] G. D. Westfall *et al.*, Phys. Rev. Lett. 37, 1202 (1976) [nuclear fireball (here for heavy-ion collisions)].
[7] A. M. Poskanzer *et al.*, Phys. Rev. Lett. 35, 1701 (1975); H. G. Baumgardt *et al.*, Z. Phys. A 273, 359 (1975) (shock waves).
[8] M. Blann, Annu. Rev. Nucl. Sci. 25, 123 (1975) (preequilibrium decay).

[9]R. D. Amado and R. M. Woloshyn, Phys. Rev. Lett. 36, 1435 (1976); H. J. Weber and L. D. Miller, Phys. Rev. C 16, 726 (1977) (recent work with preformed clusters).
[10]J. Gosset *et al.*, Phys. Rev. C 16, 629 (1977).
[11]A. G. Seamster, R. E. L. Green, and R. G. Korteling, Nucl. Instrum. Methods 145, 583 (1977).
[12]S. Jaccard of the BASQUE experimental group at TRIUMF is thanked for supplying the signals and pertinent information.
[13]T. D. Thomas, Phys. Rev. 116, 703 (1959).
[14]W. R. Frazer *et al.*, Rev. Mod. Phys. 44, 284 (1972).
[15]G. D. Westfall *et al.*, Phys. Rev. C 17, 1368 (1978).